V European Conference on Computational Fluid Dynamics
ECCOMAS CFD 2010
J. C. F. Pereira and A. Sequeira (Eds)
Lisbon, Portugal, 14–17 June 2010

FINE LARGE EDDY SIMULATION OF THE FLOW AROUND ONE AND TWO SIDE-BY-SIDE INFINITE CYLINDERS AT SUBCRITICAL REYNOLDS NUMBERS

Y. Kahil[††], S. Benhamadouche[*], P. Sagaut[††]

[*]Electricité de France - R&D Division
Fluid Mechanics, Power Generation and Environment Dept.
6, Quai Watier, 78401 Chatou Cedex, France
e-mail: sofiane.benhamadouche@edf.fr

[††]Institut Jean Le Rond d'Alembert,
Université Pierre et Marie Curie-Paris 6, 4, Place Jussieu, Paris, France
{kahil,sagaut}@lmm.jussieu.fr

Key words: Large Eddy Simulation, Circular cylinder, side-by-side cylinders, sub-critical Reynolds number

Abstract. *The flow around one and two side-by-side infinite fixed cylinders is computed using Large Eddy Simulation. The first simulations dealing with the flow around a single infinite cylinder are performed at the Reynolds numbers 3000 and 3900 and compared to experimental data and fine numerical simulations. Satisfactory quantitative results are obtained. Sensitivity studies of the solution to the mesh refinement in the wall normal and the spanwise directions, to the subgrid scale model and to the extrusion length have been carried out. The mean solution is not influenced by the extrusion length or a finer refinement in the spanwise direction. However, switching off the subgrid-scale model or coarsening the mesh in the wall normal direction have a dramatic effect on the recirculation bubble and thus on the whole velocity field. Then, a calculation is carried out for two side-by-side cylinders with a pitch ratio equal to 1.5 at a Reynolds number of 3000. The comparisons with available experimental data show a satisfactory agreement. Two shedding frequencies are detected and the deflection of the flow is clearly observed. Moreover, the bi-stability which is not reproduced experimentally, is observed during the same numerical simulation.*

1 INTRODUCTION

Fluid-elastic instabilities, wear and fatigue of steam generators tubes are a major concern for nuclear operators. Estimation of these phenomena requires the knowledge of fluid forces acting on the tubes. In order to predict these forces, fine simulations (Large Eddy Simulation or Direct Numerical Simulation) which allow obtaining large temporal spectra are required. Before dealing with multiple tubes configurations (in-line or staggered bundles in the present case), one has to focus on simpler configurations such as the flow over a single cylinder, the flow over two or three side by side cylinders, the flow over tandems of cylinders, …

The present paper deals with the numerical simulation using Large Eddy Simulation of the flow over a single and two side-by-side cylinders at sub-critical Reynolds numbers. For both cases, a literature review can be found in Parnaudeau et al.[1] and Sumners et al. [2] respectively.

After computing a standard flow over a single cylinder at Re=3000 and Re=3900, a sensitivity study to the mesh refinement, the extrusion length and the subgrid-scale model is carried out. Finally, the side-by-side configuration with a pitch ratio equal to 1.5 is computed and some quantitative and qualitative data are provided and compared to available experimental results.

2 NUMERICAL METHOD

EDF in-house open source CFD tool *Code_Saturne* is utilized herein (www.code-saturne.org). *Code_Saturne* is an unstructured collocated finite volume solver for incompressible flows using a SIMPLEC algorithm for pressure-velocity coupling, with a Rhie and Chow interpolation to avoid odd-even decoupling on structured meshes. Further details about the code and its capabilities can be found in Archambeau et al. [3]. One focuses herein on Large Eddy Simulation. The flow is assumed Newtonian and the density ρ is constant. If $\underline{\bar{u}}$ stands for the filtered velocity, the filtered Navier-Stokes equations can be written :

$$\begin{cases} \dfrac{\partial \bar{u}_i}{\partial t} + \dfrac{\partial \bar{u}_i \bar{u}_j}{\partial x_j} = -\dfrac{1}{\rho}\dfrac{\partial \bar{p}}{\partial x_i} + \nu \dfrac{\partial^2 \bar{u}_i}{\partial x_j \partial x_j} - \dfrac{\partial \tau_{ij}}{\partial x_j} \\ \dfrac{\partial \bar{u}_j}{\partial x_j} = 0 \end{cases} \qquad (1)$$

The sub-grid scale tensor $\underline{\underline{\tau}}$ has to be modeled. The dynamic Smagorinsky model based on Germano identity [4] and Lilly minimization [5] is used to take into account the small structures that are mainly dissipative. The deviatoric part of the subgrid-scale tensor is given by :

$$\tau_{ij} - \frac{1}{3}\tau_{kk}\delta_{ij} = -2\nu_t \bar{S}_{ij} = -2(C_S \bar{\Delta})^2 \|S\| \bar{S}_{ij} \qquad (2)$$

$\bar{S}_{ij}$ is the filtered strain rate tensor, $\|S\| = \sqrt{2\bar{S}_{ij}\bar{S}_{ij}}$, ν_t the subgrid-scale viscosity, $\bar{\Delta}$ the filter width and C_s the dynamic Smagorinsky constant. As the cells used in the present work are hexahedral (even if *Code_Saturne* accepts cells of any shape), one can

take $\overline{\Delta} = 2\Omega^{\frac{1}{3}}$, where Ω is the volume of a computational cell. The term $\frac{1}{3}\tau_{kk}\delta_{ij}$ is taken into account in the pressure gradient. The filter which appears in equation (1) is implicit as it is introduced by the discretization errors in space and time and by the model itself. The explicit filter which is applied to compute the dynamic constant C_s uses the neighbors which share a node with the computational cell. No averaging in the homogeneous directions (the spanwise direction in the present cases) is performed. No negative value is allowed to the subgrid-scale viscosity and the maximum value of the dynamic constant is set to 0.065 (the value used with the standard Smagorinsky model).

In the collocated finite volume approach, all the variables are located at the centres of gravity of the cells. The momentum equations are solved by considering an explicit mass flux (the three components of the velocity are thus uncoupled). A second order centred scheme in space and time is used. It is Crank-Nicolson in time with a linearized convection, and the second order Adams-Bashforth method is used for the part of the diffusion involving the transposed gradient operator, that couples the velocity components. A centred scheme is utilized for the convection operator. However, a slope test is used. When the test is positive, 1% upwinding is added to the centred scheme. The non-orthogonalities are taken into account with an implicit reconstruction technique explained in Archambeau et al. [3]. When a non-orthogonal grid is used, the matrix contains only the orthogonal contributions of the different operators. The non-orthogonal part is added to the right hand side of the transport equation (thus, inner iterations are needed for the velocity and pressure equations to make the gradient reconstruction implicit). The code has been validated with LES on several academic cases (decaying isotropic turbulence, channel flow) and industrial ones (T-junctions, combustor chamber, …) in Benhamadouche [6]. Benhamadouche and Laurence [7] also validated the approach on a staggered tube bundle configuration.

3 COMPUTATIONAL DETAILS

Two main cases have been computed. The flow over an infinite cylinder and the flow over two side-by-side cylinders of the same diameter with a pitch ration T/D=1.5. D is the diameter of the cylinders and T the distance between two centres. The computational domain and a view of the mesh for the flow over one cylinder are shown in figure 1. The size of the computational domain is $25D \times 20D \times 4D$. The length of the computational domain upstream the cylinder is equal to $10D$. This is necessary to allow the pressure field to reach an upstream asymptotic behaviour. A discussion is developed in Parnaudeau et al. [1] about the minimum spanwise length (or extrusion length) which has to be taken. πD seems to be enough. The total number of cells is equal to 13 million. 256 cells are used in the spanwise direction. This is superior to what is usually used with more accurate numerical schemes (Parnaudeau et al. [1] use for example 48 points for a spanwise length equal to πD with a sixth order compact scheme). As LES technique is very sensitive to non-orthogonal or non-conforming meshes, a fully conforming hexahedral mesh is used.

Constant boundary conditions are used at the inlet (constant velocity in space and time) and no synthetic method to generate turbulence is used. The flow is laminar upstream the cylinders. As it will be shown, the meshes are very fine at the wall, thus, no slip boundary conditions are used for the velocity and homogeneous Neumann conditions for the pressure. No wall functions have been necessary during the unsteady simulations. Periodic boundary conditions are used in the spanwise direction. The outlet conditions are standard, Dirichlet condition for the pressure and homogeneous

Neumann for the velocity. Symmetry boundary conditions are used for the upper and lower boundary faces (see figure 1).

Two Reynolds numbers have been computed, Re=3000 and the most widely used Re=3900.

The maximum CFL number is equal to 0.6. The corresponding time step is $\Delta t = 0.005\ D/U_0$. where U_0 is the bulk velocity. One flow passage corresponds to 5000 time steps. The first computation is performed over 14 flow passages using the last four passages for time and space averaging. The averaging corresponds to 20 shedding periods. This should be enough to have a reasonable uncertainty on the statistics (this of course depends on which statistic one considers). The non-dimensional mean refinements at the wall is shown on figure 2. If y and z stand respectively for the wall normal an spanwise directions, one can observe that Δy^+ and Δz^+ do not exceed 2 and 12 (this means that the maximum distance between the first computational node at the wall and the wall is around 1). The azimuthal refinement $D\Delta\theta^+/2$ does not exceed 12 as well. These are the maximum values. The wake region corresponds in figure 2 to the angles between 90° and 270°. It this region, the maximum values of Δy^+, $D\Delta\theta^+/2$ and Δz^+ are respectively 0.5, 3 and 4.

As it will be shown in the next part, the solution of the flow over two side-by-side cylinders is bi-stable what makes this case more difficult to deal with. Figure 3 shows the computational mesh which contains 25 million cells (256 cells in the spanwise direction). The same time step is used for this computation. The computation has been for the moment pushed to a physical time equal to 2500 what corresponds to 250 shedding period for one of cylinders and to 1000 shedding period for the other one (as it will be shown later, the shedding frequency changes compared to the flow around one cylinder). When statistical quantities are shown, they are obtained on one stable situation over a physical time equals to 400 s (respectively 40 and 160 shedding periods). Figure 4 shows the refinements at the wall for the two cylinders. The asymmetry of the flow can be observed on this figure. The refinements in the spanwise and azimuthal directions are of the same order as for the single cylinder. The mesh is finer in the wall normal direction in the present case.

HPC calculations have been carried out using 1024 or 2048 processors on EDF BlueGene/L and BlueGene/P supercomputers. One needs about 4.5 days (resp. 5 days) for 350 (resp. 400) physical seconds for the isolated cylinder (resp. side-by-side configuration) on 1024 (resp. 2048) processors.

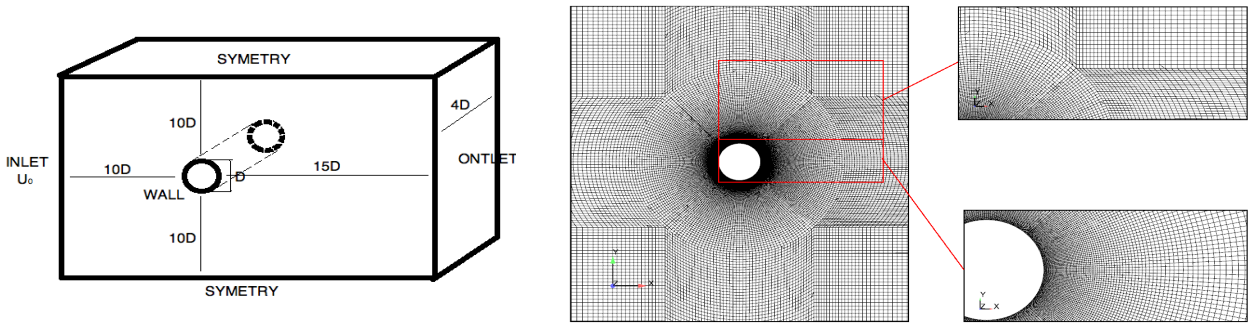

Figure 1: The computational domain and the mesh for the flow over one cylinder.

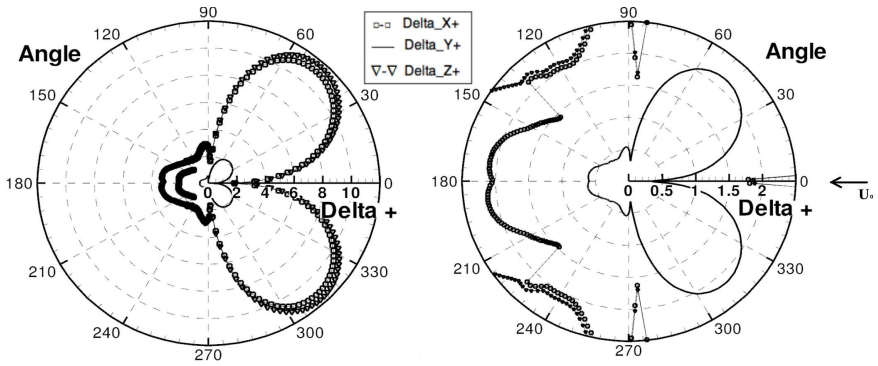

Figure 2: Near wall resolution for the flow around one cylinder (right: zoom of the image on the left, Δx^+ is actually $D\Delta\theta^+/2$).

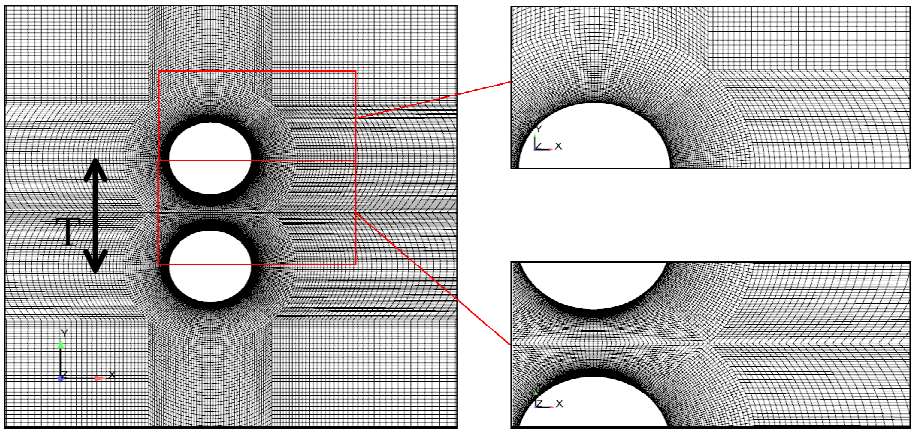

Figure 3: The mesh for the flow over two side-by-side cylinders at Re=3000.

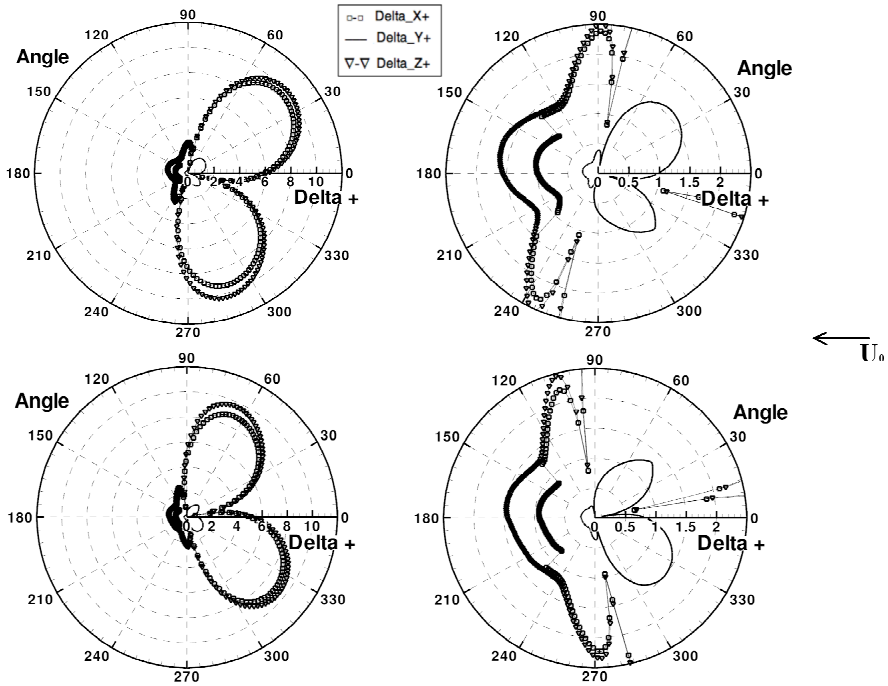

Figure 4: Near wall resolution for two side-by-side cylinders.

4 RESULTS AND DISCUSSION

4.1 Flow around one circular cylinder at Re = 3000 and Re=3900

Both Reynolds numbers Re=3000 and Re=3900 have been computed. The first Reynolds number has been performed to have a reference solution for the flow over two side-by-side cylinders. The second Reynolds number is widely used in the literature.

4.1.1. Mean statistics

Figure 5 gives the streamwise velocity along the symmetry axis y=0 compared to two experimental results and to the DNS of Rodi and Wissink [8]. This profile allows to define the recirculation length. As it can be seen, the profile is in very good agreement with Parnaudeau et al. [1] experiment and the DNS. Lourenko and Shih [9] experiment exhibits a shorter recirculation region which might be due to possible upstream turbulence. Parnaudeau et al. [1] checked in their experiment that they do not exceed a turbulence intensity of 0.4% at the entrance of the testing zone. Note that the profile obtained with Re=3000 exhibits a longer recirculation zone comparable to the one obtained by Rodi and Wissink [8] with Re=3300.

Table 1 gives mean integral quantities compared to available numerical and experimental results. All the results are in relatively good agreement with the references. Note that the recirculation length in the present case is higher than the others and closer to the one obtained recently by Parnaudeau et al. [1]. Figures 6 and 7 give the mean streamwise and normal velocity components at three locations in the wake region compared to two experiments and to a DNS. A U shape profile is observed for the streamwise velocity. This is coherent with the available simulations in the literature. The V shape measured by Lourenco and Shih [9] might be due to an uncertainty in the experimental setup. Figures 8 to 10 give the turbulent mean quantities compared to the most relevant experiment (from Parnaudeau et al. [1]) at three locations in the wake region. The agreement is very satisfactory although the numerical method is only second order in space. Figures 11 shows the mean pressure coefficient distribution around the cylinder. The pressure coefficient is in good agreement with Norberg experiment [10] which has been performed at Re = 4020. The Cp value is not very sensitive to the Reynolds number. Finally, figure 12 shows the power spectra obtained with the lift and drag coefficients. The results are of the same order as the one obtained in the literature, a Strouhal number of 0.21 is obtained for the lift and around 0.4 for the drag.

	Present LES	Breuer[11] LES	Kravchenko[12] LES	Wissink[8] DNS	Experiments	
$<C_D>$	1.007	1.016	1.040	--	0.98±0.05	Norberg[10]
$<C_L>$	-0.0005	--	--	--	--	
$<Cp_{back}>$	-0.9	-0.94	-0.94	--	-0.9±0.05	Norberg[10]
θ (°)	87	87.3	88	87.3	85±2	Cardell[13]
Lr/D	1.46	1.37	1.35	--	1.33±0.2	Cardell[13]
St	0.213	0.215	0.210	0.214	0.215±0.005	Cardell[13]
Ur_{max}/U_0	-0.32	-0.23	-0.37	--	-0.24±	Lourenko[9]

Table 1: Mean integral quantities compared to experiments and computations.

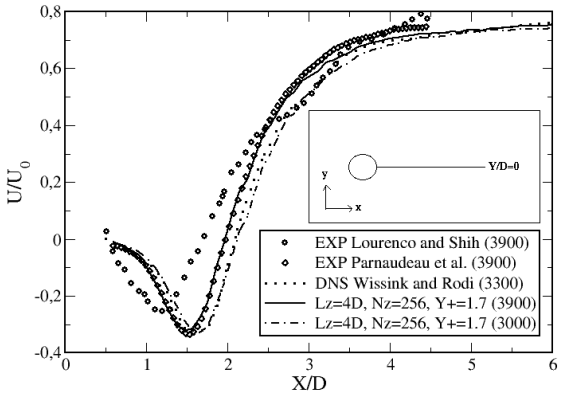

Figure 5 : Mean streamwise velocity along y=0.

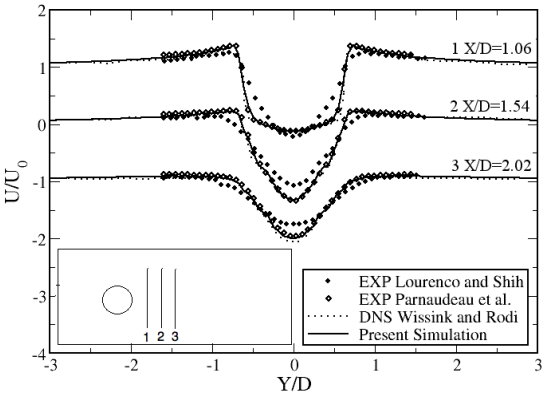

Figure 6 : Mean streamwise velocity in the wake.

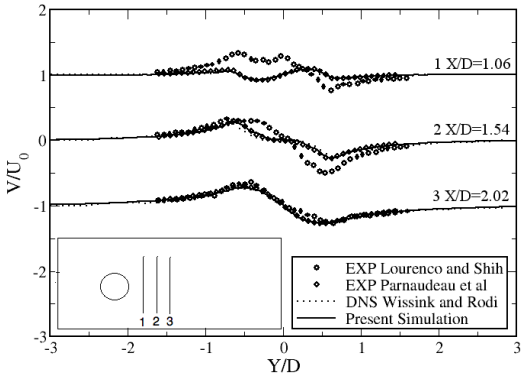

Figure 7 : Mean normal velocity in the wake.

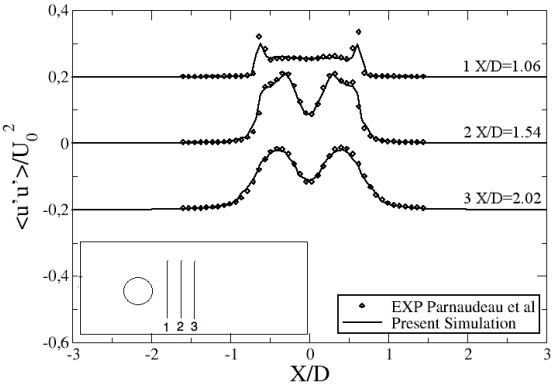

Figure 8 : Streamwise fluctuations in the wake.

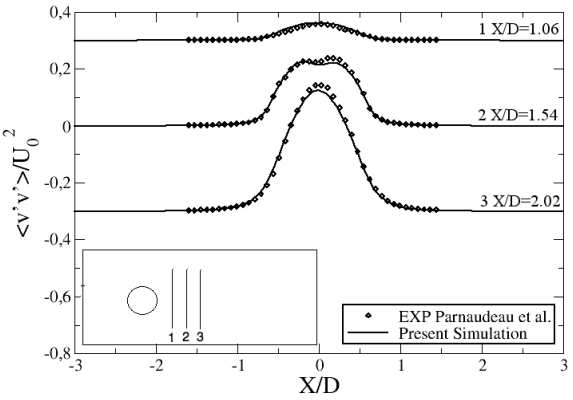

Figure 9 : Normal fluctuations in the wake.

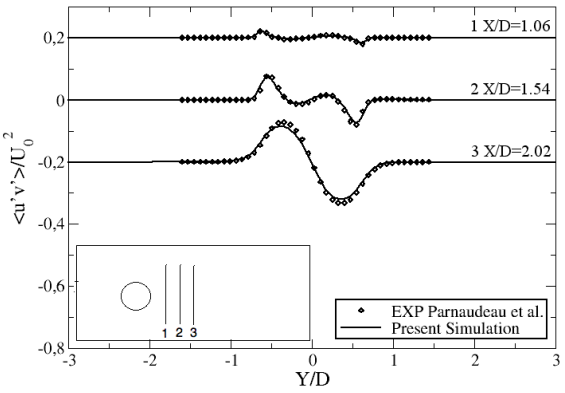

Figure 10 : Covariance in the wake.

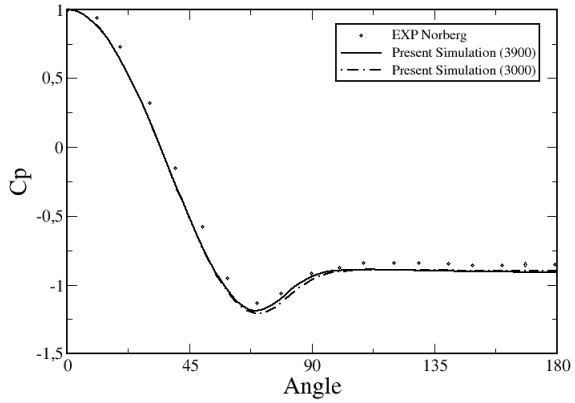

Figure 11 : Cp coefficient.

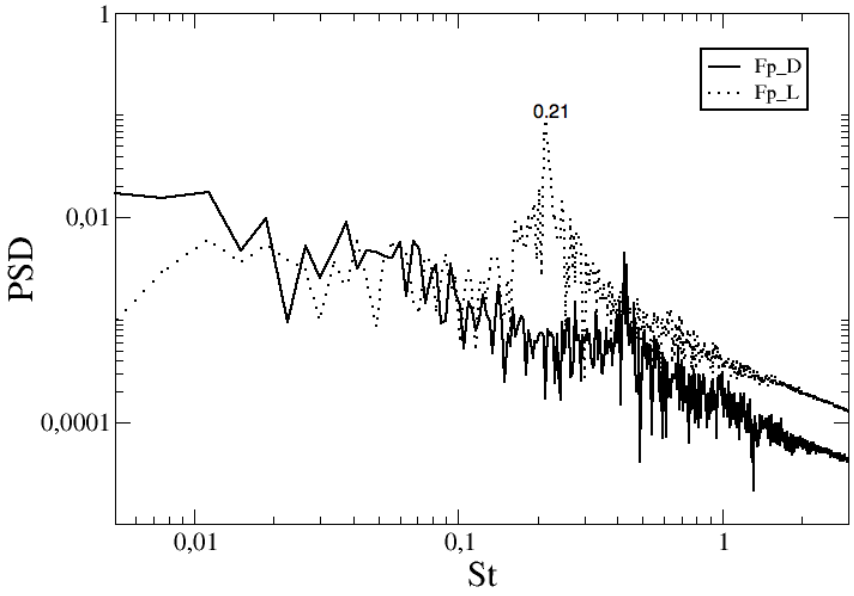

Figure 12 : Power spectra of the lift and drag coefficients.

4.1.2. Sensitivity to the model, the spanwise length and the mesh refinement

Figure 13 gives the mean streamwise velocity profile along the axis y=0 for a calculation using 512 nodes in the spanwise direction and an extrusion length equal to 8*D* (the Reynolds number is equal to 3000, that is why the experimental data are not plotted). No differences are observed concerning this profile if one compares it to the reference case (256 nodes and an extrusion length of 4*D*). Figure 14 shows the effect of switching off the subgrid-scale model. A dramatic affect on the recirculation length is observed. The results are also surprisingly in very good agreement with Lourenco and Shih experiment [9]. No satisfactory explanation concerning this issue has been found for the moment. Unfortunately the first tests on the mesh refinement have been made without any subgrid scale model. Figure 14 shows the sensitivity to the mesh refinement in the spanwise and wall normal directions. Although the spanwise refinement has a very small effect (only small variations are observed), the refinement in the wall normal direction plays a major role (the results are very different from those obtained with a finer mesh in the wall normal direction, the recirculation region becomes very small).

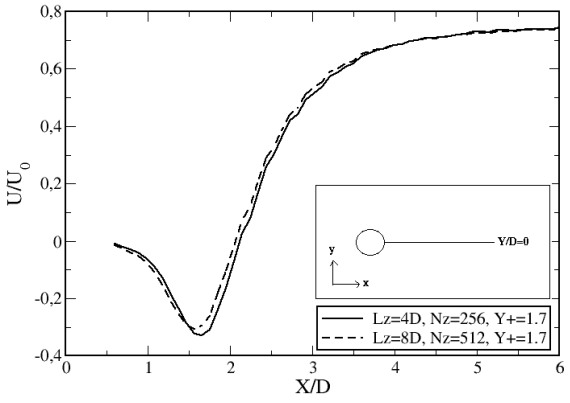

Figure 13 : Mean streamwise velocity along y=0, sensitivity to the spanwise direction length.

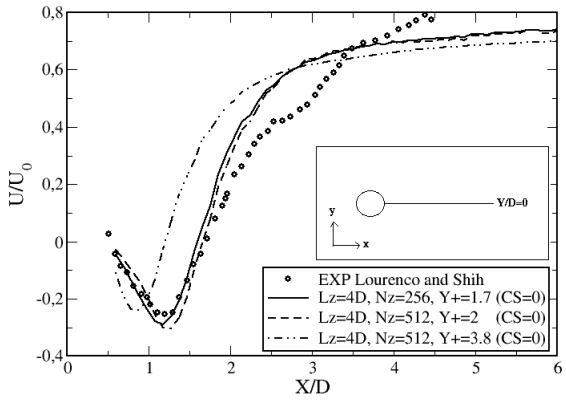

Figure 14 : Mean streamwise velocity along y=0, sensitivity to the model and to the mesh refinement.

4.2 Flow around side-by-side cylinders at Re = 3000 with T/D=1.5

The flow over two side-by-side cylinders has been computed with a pitch to diameter ratio *T/D* = 1.5 and at a Reynold number Re=3000. The asymmetry of the flow has been observed experimentally by several authors and a deflection angle going from 3° to 22° is observed in the experiments of Sumners et al. [2]. However, the bi-stable behavior has not been observed experimentally to the authors knowledge. In the present numerical simulation, the bi-stable behavior is observed as it is shown in figure 15. Figure 19 shows the time evolution of the pressure lift force. Two plateaux are observed for the two cylinders and this indicates the bi-stable behavior. The physical computational time is still not long enough to conclude whether the change from a stable regime to another is regular (if it occurs at a given frequency) or random. The first two computed periods given in figure 19 indicate that the change is not periodic. Due to this difficulty which does not occur experimentally, one has to take care while averaging. Special care has thus been taken to average the main flow quantities over a stable regime. 400 physical seconds are used for averaging (first plateau of figure 19). Figure 16 gives the diagonal components of the Reynolds stress tensor and the kinetic

energy. The deflection of the flow is clearly visible. The behavior of the lower cylinder is totally different from the single cylinder configuration. An extended wake region is observed downstream the lower cylinder and a high turbulent activity downstream the upper one. Unfortunately no fine experimental data are available to the authors knowledge in order to perform fine comparisons. Figure 17 gives the pressure coefficient. The asymmetry is again clearly visible as the high pressure zone on the lower cylinder is shifted. The upper cylinder behaves like the single case cylinder. Figure 18 gives the power density spectra of the lift coefficient for both cylinders. Whereas the upper cylinder exhibits a first peak at a Strouhal number of 0.1, both cylinders show a peak at a Strouhal number of 0.4. This is characteristic of the existence of two vortex shedding. These results are supported by the experimental results of Sumners et al. [2]. Finally, one can notice in figure 19 that the oscillation magnitude of lift force for both cylinders is lower than the one obtained in the single cylinder configuration. More investigations on the present test-case are needed. The quantity of numerical data is huge and finer information such as inter-spectra correlations can be obtained.

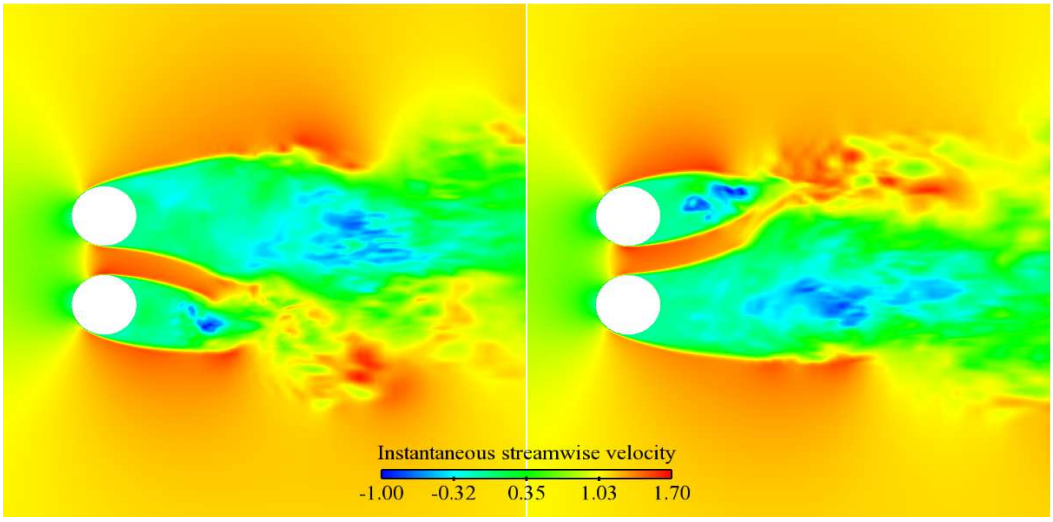

Figure 15 : Instantaneous streamwise velocity at the two stable regimes.

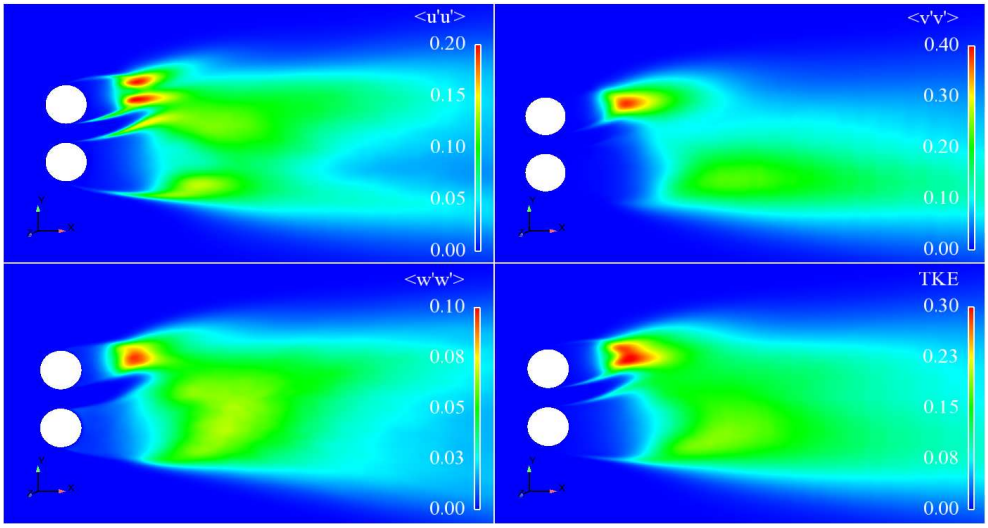

Figure 16 : Turbulent quantities when the flow is deflected to the top (top left : streamwise fluctuations, top right : normal fluctuations, bottom left : spanwise fluctuations, bottom right : turbulent kinetic energy).

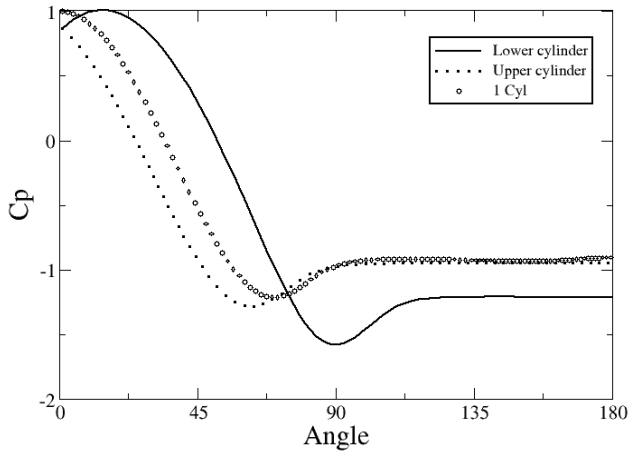

Figure 17 : Cp coefficient (side-by-side configuration)

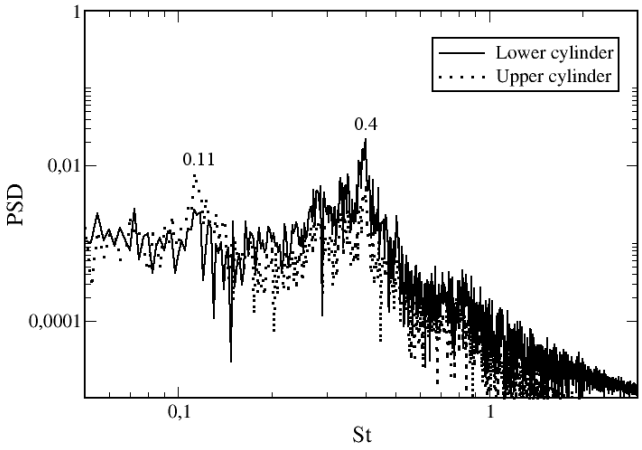

Figure 18 : Power spectra of the lift coefficient (side-by-side configuration).

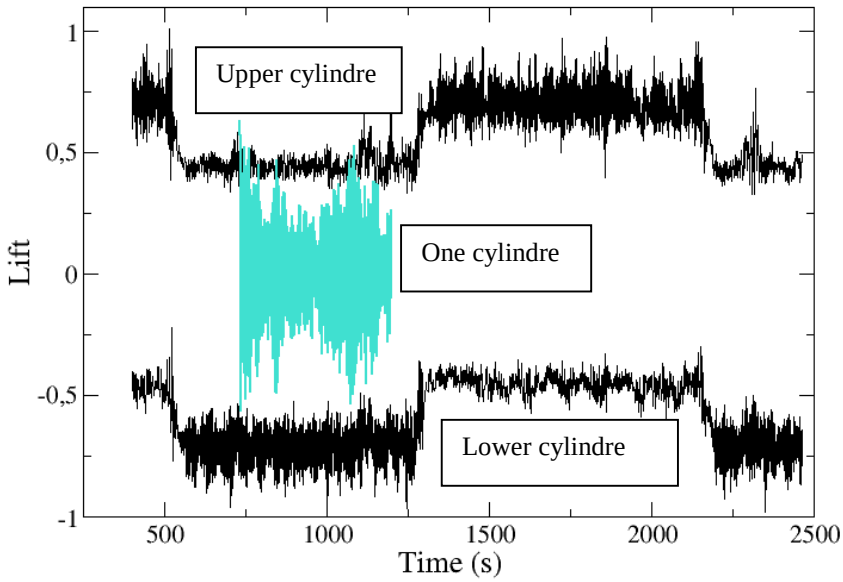

Figure 19 : Time evolution of the lift force (side-by-side configuration).

6 CONCLUSIONS

The flow around one and two side-by-side infinite fixed cylinders is computed using Large Eddy simulation with the in-house EDF unstructured CFD tool *Code_Saturne*. The first simulation dealing with the flow around an infinite cylinder is performed at the Reynolds numbers 3000 and 3900 and compared to experimental data and fine numerical simulations. Satisfactory quantitative results are obtained concerning both integral and local quantities. Sensitivity studies of the solution to the mesh refinement in the wall normal and the spanwise directions, to the subgrid scale model and to the extrusion length have been carried out. The mean solution is not influenced by the extrusion length or the refinement in the spanwise direction. However, switching off the subgrid-scale model or coarsening the mesh in the wall normal direction have a dramatic effect on the recirculation bubble and thus on the overall solution. A computation is then carried out for two side-by-side cylinders with a pitch ratio equal to 1.5 at a Reynolds number of 3000. The comparisons with available experimental data show a satisfactory agreement. The two shedding frequencies are detected and the deflection of the flow is clearly observed. Moreover, the bi-stability which has not been reproduced experimentally is observed during the same numerical simulation.

REFERENCES

[1] P. Parnaudeau, J. Carlier, D. Heitz, and E. Lamballais, Experimental and numerical studies of the flow over a circular cylinder at Reynolds number 3900. *Phys. Fluids.* **20**, 085101 (2008)

[2] D. Sumners, S.S.T. Wong, S.J. Price, M.P. Paidoussis, Fluid behaviour of side-by-side circular cylinders in steady cross-flow. *Journal of Fluids and Structures.* **13**, pp. 309-338 (1999)

[3] F. Archambeau, N. Méchitoua, and M. Sakiz, "*Code_saturne*: a finite volume code for the computation of turbulent incompressible flows – industrial applications", *Int. J. Finite Volumes.* **1**, (2004)

[4] M. Germano, U. Piomelli, P. Moin and W. Cabot. A dynamic subgrid-scale eddy viscosity model. *Phys. Fluids*, **3(7)**. pp, 1760–1765 (1991)

[5] D. Lilly. A proposed modification of the germano subgrid-scale closure method. *Phys. Fluids*. **4,** pp. 633–635 (1992)

[6] S. Benhamadouche, "Large eddy simulation with the unstructured collocated arrangement", *PhD Thesis*, The University of Manchester (2006)

[7] S. Benhamadouche and D. Laurence, "LES, coarse LES, and transient RANS comparisons on the flow across tube bundle", *Int. J. Heat and Fluid Flow*. **4**, pp. 470-479 (2003)

[8] J.G. Wissink, W. Rodi, Numerical study of the near wake of a circular cylinder, *Int. J. Heat and Fluid Flow.* **29,** pp. 1060–1070 (2008)

[9] L.M. Lourenco, C. Shih, Characteristics of the plane turbulent near wake of a circular cylinder, a particle image velocimetry study, Published in Beaudan and Moin (1994)

[10] C. Norberg, Effects of Reynolds number and low-intensity free stream turbulence on the flow around a circular cylinder, Publ. No. 87/2, Department of Applied Thermoscience and Fluid Mech., Chalmers University of Technology, Gothenburg, Sweden, (1987)

[11] M. Breuer, Large eddy simulations of the subcritical flow past a circular cylinder : numerical and modelling aspects. *Int. J. Numer. Meth. Fluids.* **28**, pp. 1281–1302 (1998)

[12] A.G. Kravchenko, P. Moin, Numerical studies of flow around a circular cylinder at Re 3900. *Phys. Fluids.* **12**, pp. 403–417 (2000)

[13] G. S. Cardell, Flow past a circular cylinder with a permeable splitter plate. *Ph.D. Thesis*, Graduate Aeronautical Laboratory, California Inst. Of Technology (1993)